

## Exciton Regeneration at Polymeric Semiconductor Heterojunctions

Arne C. Morteani, Paiboon Sreearunothai, Laura M. Herz,\* Richard H. Friend, and Carlos Silva†

*Cavendish Laboratory, University of Cambridge, Madingley Road, Cambridge CB3 0HE, United Kingdom*

(Received 16 October 2003; published 18 June 2004)

Control of the band-edge offsets at heterojunctions between organic semiconductors allows efficient operation of either photovoltaic or light-emitting diodes. We investigate systems where the exciton is marginally stable against charge separation and show via *E*-field-dependent time-resolved photoluminescence spectroscopy that excitons that have undergone charge separation at a heterojunction can be efficiently regenerated. This is because the charge transfer produces a geminate electron-hole pair (separation 2.2–3.1 nm) which may collapse into an exciplex and then endothermically ( $E_A = 100$ –200 meV) back transfer towards the exciton.

DOI: 10.1103/PhysRevLett.92.247402

PACS numbers: 78.55.Kz, 73.20.-r, 73.50.Pz, 78.66.Qn

Efficient optoelectronic devices fabricated with semiconductor polymers often employ heterojunctions between two components in which both the electron affinity and ionization potential are higher in one material than in the other (“type II” heterojunctions; see inset in Fig. 1). This configuration is commonly used in photovoltaic diodes to achieve charge generation at the heterointerface [1–3]. Typical devices involve a thin film of a blend of hole-accepting and electron-accepting polymers sandwiched between two electrodes. However, some type II polymer blends show low photocurrents and high luminescence quantum yields, leading to very efficient light-emitting diodes [4–7].

The high luminescence quantum yield is commonly rationalized by the proposition that excitons can be stable at the heterojunction if their Coulombic binding energy is higher than the band-edge offsets [4]. In this case, the only process that might occur when an exciton encounters the heterojunction is energy transfer from the material with the larger band gap to the other component. This picture classifies type II heterojunctions into those above and those below a charge-separation threshold, producing high photocurrents or luminescence quantum yields, respectively. This simple classification is incomplete because even systems that show high luminescence efficiencies often also show significant charge generation (see below). By considering the dependence of photoluminescence spectra and dynamics on applied electric field, we develop here an alternative, unified description of the excitation dynamics at the polymer heterojunction. We show that in *all* blends the exciton first dissociates at the heterojunction and forms an interfacial geminate charge pair. However, geminate-pair recombination via an intermediate heterojunction state (termed an exciplex) can regenerate the bulk exciton. These circular transitions between the different excited states at the heterojunction are driven by thermal energy, and a fine balance of the kinetics determines the net charge-separation and photoluminescence yields.

Bulk excitons show relatively strong Coulombic binding (of order 0.5 eV [4,8]) and can be trapped at the

heterojunction, acquiring some charge-transfer character. Such excitations are termed exciplexes when seen in isolated donor-acceptor systems and are characterized by featureless, redshifted emission spectra and long radiative decay times [9]. Recently, we have shown that exciplex states form in blends of poly(9,9-dioctylfluorene-co-benzothiadiazole) (F8BT) with poly(9,9-dioctylfluorene-co-bis-N,N-(4-butylphenyl)-bis-N,N-phenyl-1,4-phenylenediamine) (PFB), and F8BT with poly(9,9-dioctylfluorene-co-N-(4-butylphenyl)diphenylamine) (TFB) (see Fig. 2 for molecular structures) and that these exciplex states can undergo endothermic energy transfer to form a bulk F8BT exciton [7]. Here we investigate films of PFB:F8BT and TFB:F8BT spin coated from a common chloroform solution. In general, there is substantial demixing of the two polymers through spinodal decomposition during drying, but, under the rapid drying conditions achieved here, there is more limited demixing (of the order of 10 nm [2]), resulting in a large interfacial area of contact between the two polymers. Note that PFB:F8BT blends can display high charge-separation yields (4% photocurrent external quantum efficiency) and low electroluminescence efficiencies (<0.64 lm/W), whereas the TFB:F8BT system displays low photocurrents (we find 82% lower short-circuit current than in PFB:F8BT at 457 nm excitation) but very high electroluminescence efficiencies (up to 19.4 lm/W) [7,10]. Hence, these blends are good examples for the contrasting properties of type II polymer heterojunctions as described above.

For all measurements, polymer blends (mass ratio 1:1) were spin coated from a common chloroform solution onto oxygen-plasma-treated indium-tin oxide (ITO) substrates to form 170 nm thin films. Ca electrodes (60 nm) were then deposited by thermal evaporation and encapsulated by a 300 nm Al layer. All devices were fabricated under a  $N_2$  atmosphere. An electric field was applied by reverse biasing the device to prevent charge injection (ITO negative with respect to Ca). Quasi-steady-state photoluminescence (PL) quenching measurements were taken by exciting the sample with a cw  $Ar^+$  laser (457 nm)

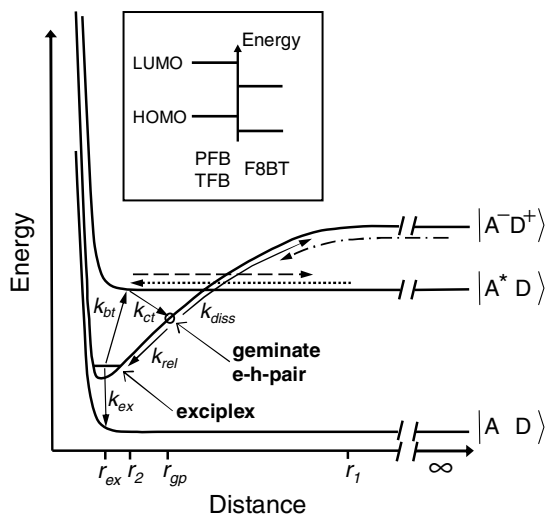


FIG. 1. Potential energy diagram describing the energetics and kinetics at type II polymer heterojunctions. The energetic order of  $|A^-D^+\rangle_{r=\infty}$  and  $|A^*D\rangle_{r=\infty}$  may be reversed for PFB:F8BT vs TFB:F8BT. The inset shows the band offsets at a type II heterojunction (see also [7]).

through the ITO. The resulting PL was imaged through a monochromator onto a Si photodiode. A modulated voltage was applied to the device and changes in PL due to the applied electric field  $\Delta PL$  were detected using a lock-in amplifier referenced to the modulation frequency (225 Hz). The total PL intensity was measured by mechanical modulation of the laser excitation. The results reported here are independent of modulation frequency and excitation power. Time-resolved PL measurements were performed using time-correlated single photon counting (TCSPC) and photoluminescence up-conversion (PLUC) spectroscopies with 70 ps and 300 fs time resolution, respectively. Our TCSPC and PLUC setups are described elsewhere [7,11]. All measurements were taken in continuous-flow He cryostats (Oxford Instruments OptistatCF) under inert conditions. Finally, PL efficiency measurements were performed on simple polymer thin films spin coated on Spectrosil substrates using an integrating sphere coupled to an Oriel InstaSpec IV spectrograph and excitation with the same  $Ar^+$  laser as above.

Figure 2(a) compares the PL spectrum of a diode made with blended PFB:F8BT with that of pure F8BT. Redshifted exciplex emission, in addition to bulk F8BT contribution (i.e., the F8BT-only spectrum), is evident in the blend film. (Neither PFB nor TFB are excited at 457 nm [10].) Also shown in the same figure is the  $-\Delta PL$  spectrum taken by applying 10 V bias across the device. The electric field preferentially quenches the exciplex contribution in the red part of the spectrum ( $>50\%$  quenching for wavelengths  $>650$  nm). Quenching of the F8BT exciton emission is also observed but decreases with decreasing temperature, as demonstrated in Fig. 2(b). Similar phenomena are observed in the TFB:F8BT diode [Figs. 2(c) and 2(d)], although the rela-

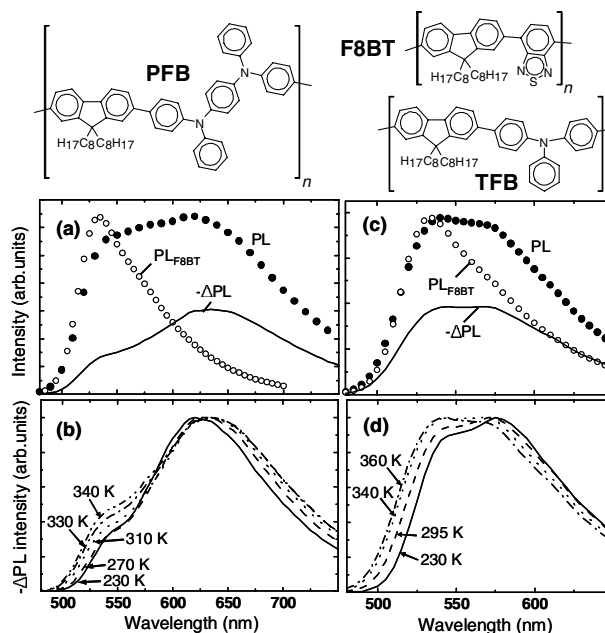


FIG. 2. (a) Photoluminescence intensity (PL, solid circles) and reduction of photoluminescence intensity due to an applied reverse bias of 10 V ( $\Delta PL$ , continuous line) for a PFB:F8BT blend device at 340 K. PL and  $-\Delta PL$  are plotted in the same scale and reflect their relative intensities. (b)  $\Delta PL$  spectra (at 10 V) from the same device as in (a) at different temperatures. (c) PL (solid circles) and  $\Delta PL$  at a reverse bias of 15 V (continuous line) for a TFB:F8BT blend device at 340 K. (d)  $\Delta PL$  spectra from the same device as in (c) at different temperatures. For comparison, the PL spectrum from an F8BT-only device (open circles) is plotted in both parts (a) and (c). The structures of PFB, F8BT, and TFB are also shown.

tive contribution of F8BT bulk emission is higher in the same temperature range. In contrast to the blends, pure F8BT does not show PL quenching (integrated  $\Delta PL/PL \ll 1\%$ ) and only Stark shifts by  $<1$  nm at these fields.

If the PL quenching arises from field-assisted dissociation of an emissive state, its luminescence decay rate should be field dependent. Figure 3(a) shows TCSPC measurements at 640 nm from a PFB:F8BT diode with different applied voltages. All curves consist of an instrument-limited decay and a slow, roughly mono-exponential decay with a  $40 \pm 5$  ns time constant. The two components are assigned to the bulk exciton and the exciplex state, respectively [7]. Exciplex generation occurs within  $\sim 1$  ns and its generation efficiency is strongly field dependent, while its decay constant shows no significant variation with applied field. Therefore, an exciplex precursor must be quenched by the field. To investigate the field dependence on the bulk exciton decay rate, we have performed field-dependent PLUC measurements. The results are displayed in Fig. 3(b). The exciton decay dynamics are not field dependent [12]. Therefore, a dark intermediate state must be dissociated by the field. We postulate that this state is an interfacial geminate

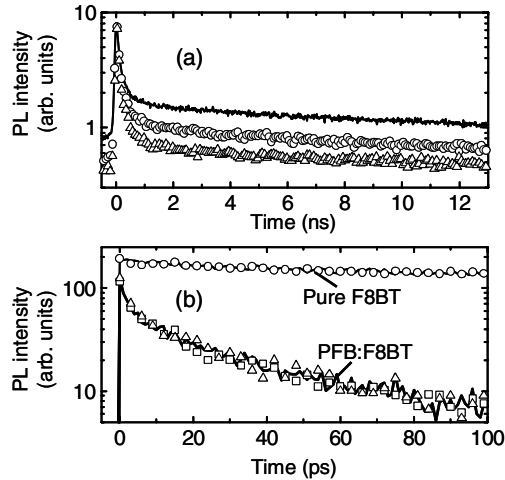


FIG. 3. (a) Photoluminescence decay measured using TCSPC (excitation: 407 nm,  $<4$  nJ/cm<sup>2</sup>; detection: 640 nm) from a PFB:F8BT device at room temperature under 0 V (continuous line), 13 V (circles), and 30 V (triangles) applied reverse biases. (b) PLUC measurements (excitation: 405 nm, 42 nJ/cm<sup>2</sup>; detection: 550 nm) from a similar device at 0 V (continuous line), 5 V (squares), and 12.5 V (triangles) reverse bias. For comparison, data for a device with pure F8BT at 0 V (continuous line) and 12 V (circles) are also plotted.

polaron pair that follows charge transfer from the bulk exciton [13–16].

To estimate the electron-hole separation within this geminate pair  $r_{gp}$ , we have investigated the field-dependent changes in PL intensity (Fig. 4). Neglecting the effects of energetic disorder [17] and of a possible interfacial dipole layer [16], geminate-pair dissociation in electric fields is most easily described within the Onsager model [18], which yields the dissociation probability  $f_{\epsilon}(r_{gp}, T, F) = f(F)$  of bulk geminate pairs in a medium with dielectric constant  $\epsilon$ , under an applied field  $F$  and at temperature  $T$  [19]. Since the only material parameter is the dielectric constant, which we approximate to be 3.5 for all polymers, Onsager theory should also be applicable to geminate pairs at the interface. The field-dependent relative reduction of the geminate-pair population  $n_{gp}$  is given by  $-(\Delta n_{gp}/n_{gp}) = [f(F) - f(0)]/[1 - f(0)]$ . Figure 4 plots  $-(\Delta PL/PL)$  versus electric field [20] at various temperatures for PFB:F8BT and TFB:F8BT devices (measured in the red part of the spectrum where exciton emission is insignificant). Plotted in the same graph are simulations of  $-(\Delta n_{gp}/n_{gp})$  using a  $\delta$ -function distribution for  $r_{gp}$ . The simple model fits the data satisfactorily, which supports the assumption of a geminate-pair intermediate prior to exciplex formation and yields  $r_{gp} \approx 3.1$  nm (PFB:F8BT) and  $r_{gp} \approx 2.2$  nm (TFB:F8BT). The large separation is probably caused by polaron-pair thermalization following the initial charge-transfer step [13,18].

We now return to the  $\Delta PL$  spectra in Fig. 2, which contain bulk F8BT components that are not due to electric-

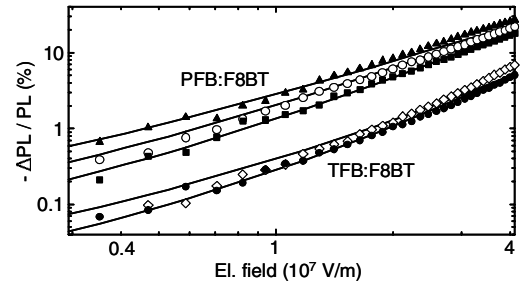


FIG. 4. Relative electric field quenching of the PFB:F8BT and TFB:F8BT exciplex photoluminescence intensities (measured at 700 and 580 nm, respectively), in the same devices as in Fig. 2, versus electric field at 230 K (solid squares), 250 K (open and solid circles), 290 K (solid triangles), and 295 K (open diamonds). The solid lines through the data are Onsager simulations (parameters for PFB:F8BT:  $\epsilon = 3.5$ ,  $r_{gp} = 3.0$  nm at  $T = 230$  K and 3.1 nm at 250 and 290 K; for TFB:F8BT:  $\epsilon = 3.5$ ,  $r_{gp} = 2.3$  nm at  $T = 250$  K and 2.2 nm at 295 K).

field-promoted dissociation of those states as was shown above. The zero-field steady-state photoluminescence is due to three different excited-state populations: (i) “primary” excitons, generated in the bulk by the laser excitation; (ii) exciplexes, generated via energy transfer from bulk excitons; and (iii) “secondary” excitons, generated via endothermic back transfer from the exciplexes [7]. Since the exciplex density is reduced by application of an electric field, there is less secondary exciton generation, and, hence, the observed  $\Delta PL$  contains an excitonic contribution. Further evidence for this hypothesis is provided by the temperature dependence of the  $\Delta PL$  spectra shown in Figs. 2(b) and 2(d) [21]. The ratio of secondary excitons to exciplexes is found to follow an Arrhenius function with activation energy  $200 \pm 50$  meV (PFB:F8BT) and  $100 \pm 30$  meV (TFB:F8BT). These activation energies are consistent with those values extracted with our previous TCSPC measurements [7].

Figure 1 summarizes the above findings. The potential energy curves represent the ground state ( $|AD\rangle$ ), the exciton residing on F8BT ( $|A^*D\rangle$ ), and the electron and the hole residing in the respective component across the heterojunction ( $|A^-D^+\rangle$ ), where A and D symbolize the acceptor (F8BT) and the donor (PFB or TFB), respectively. The abscissa represents the intermolecular distance, i.e., either the distance of the exciton from the interface or the separation of the geminate polarons. The exciplex state is then located in the minimum of the  $|A^-D^+\rangle$  potential. When the system is photoexcited, an exciton is generated at a certain distance  $r_1$  from the heterojunction. It then diffuses to a distance  $r_2$  (dotted arrow), where it dissociates and an interfacial geminate electron-hole pair is formed with rate constant  $k_{ct}$ . This geminate pair can either dissociate ( $k_{diss}$ ) or relax into the luminescent exciplex state ( $k_{rel}$ ). The ratio  $k_{diss}/k_{rel}$  is strongly field dependent and determines the degree of luminescence quenching. The exciplex state can then

either decay ( $k_{\text{ex}}$ ) or back transfer to a bulk exciton in F8BT ( $k_{\text{bt}}$ ) but is itself too strongly bound to dissociate under the field. We note that the transition from geminate pairs to excitons via  $k_{\text{rel}} \rightarrow k_{\text{bt}}$  represents a novel mechanism for geminate-pair recombination at polymeric heterojunctions. The secondary excitons produced might enter the cycle again or diffuse away from the heterojunction (dashed arrow) and decay. The model is also applicable to electrical excitation, where the excited state is produced via charge injection (dashed-dotted arrow). The regeneration of the exciton via the thermally driven circular process  $k_{\text{ct}} \rightarrow k_{\text{rel}} \rightarrow k_{\text{bt}}$  means that, even though charge transfer occurs, the excitation energy might eventually still be emitted in the form of bulk exciton luminescence.

An estimate of the contribution of the regeneration process to the PL of the blend can be derived by normalizing the  $\Delta\text{PL}$  spectrum to the PL spectrum at higher wavelengths where the emission is due solely to exciplexes. We assume that this renormalized  $\Delta\text{PL}$  then represents the contribution of exciplex and secondary exciton emission to the total PL. We infer thereby that, at room temperature in the PFB:F8BT blend,  $\sim 20\%$  of the visible emission comes from primary excitons. In TFB:F8BT we find a primary exciton contribution of  $< 2\%$ , which implies that  $> 98\%$  of the excitons undergo charge transfer at a heterojunction. Despite that, the relative PL quenching with respect to pure F8BT is only  $< 57\%$  (PL yield of F8BT 80%, of TFB:F8BT 35%) indicating the great importance of the exciton regeneration mechanism. Secondary exciton and exciplex emission maintain a high PL yield in spite of most excitons encountering a heterojunction. On the other hand, the PFB:F8BT PL yield is only 4%, consistent with large geminate-pair dissociation and low back-transfer efficiency, i.e., with low “regeneration efficiency.”

In summary, we have developed a comprehensive description of the excitonic and electronic processes at type II polymer heterojunctions that support exciplex formation. The two blends studied here represent important examples for efficient charge generation on the one hand and high luminescence yields on the other and, in this sense, represent the two extremes of type II heterojunctions found in common semiconductor polymer blends. The very different behavior was shown to arise from different geminate-pair separations (3.1 vs 2.2 nm) and back-transfer activation energies (200 vs 100 meV), which affect strongly the kinetics between the states involved. We note that both thermalization distance as well as activation energy are generally expected to be larger for larger band-edge offsets between the two polymers and that this provides the link to the classification scheme described in the introduction [4]. Given that excited-state electronic dimers are commonly observed in polymeric semiconductors [22], we consider exciplex formation and exciton regeneration to also be general phenomena at type II polymeric heterojunctions. As shown in this Letter, the central role of these dynamics

is not directly evident from steady-state PL measurements if back transfer is efficient.

In photovoltaic operation the collapse of the geminate pair into the exciplex provides an unwanted loss channel. We suggest that optimized interfaces require not only large band-edge offsets to enable large thermalization distances ( $r_{\text{gp}}$ ) but also inhibited exciplex stabilization. This can be achieved by increasing intermolecular distances and decreasing configurational relaxation [9].

This work was supported by the EPSRC. C. S. acknowledges additional financial support from the EPSRC through its ARF scheme. A. C. M. acknowledges support from the Gates Cambridge Trust. We are grateful to N. C. Greenham and A. S. Dhoot for valuable discussions.

---

\*Current address: Clarendon Laboratory, University of Oxford, Parks Road, Oxford OX1 3PU, United Kingdom.

†Corresponding author.

Email: cs271@cam.ac.uk

- [1] J. J. M. Halls *et al.*, Nature (London) **376**, 498 (1995).
- [2] A. C. Arias *et al.*, Macromolecules **34**, 6005 (2001).
- [3] C. J. Brabec, N. S. Sariciftci, and J. C. Hummelen, Adv. Funct. Mater. **11**, 15 (2001).
- [4] J. J. M. Halls *et al.*, Phys. Rev. B **60**, 5721 (1999).
- [5] Y. Cao *et al.*, Nature (London) **397**, 414 (1999).
- [6] L. C. Palilis *et al.*, Synth. Met. **121**, 1729 (2001).
- [7] A. C. Morteani *et al.*, Adv. Mater. **15**, 1708 (2003).
- [8] S. Alvarado *et al.*, Phys. Rev. Lett. **81**, 1082 (1998).
- [9] A. Weller, in *The Exciplex*, edited by M. Gordon and W. Ware (Academic, New York, 1975), pp. 23–38.
- [10] H. J. Snaith *et al.*, Nano Lett. **2**, 1353 (2002).
- [11] G. R. Hayes *et al.*, Phys. Rev. B **52**, 11 569 (1995).
- [12] We note that field-assisted exciton dissociation has been seen in a related polyfluorene at higher fields [see T. Virgili *et al.*, Phys. Rev. Lett. **90**, 247402 (2003)].
- [13] M. Yokoyama *et al.*, J. Chem. Phys. **75**, 3006 (1981).
- [14] M. W. Wu and E. M. Conwell, Chem. Phys. **227**, 11 (1998).
- [15] N. Ohta, Bull. Chem. Soc. Jpn. **75**, 1637 (2002).
- [16] V. I. Arkhipov, P. Heremans, and H. Bässler, Appl. Phys. Lett. **82**, 4605 (2003).
- [17] V. R. Nikitenko, D. Hertel, and H. Bässler, Chem. Phys. Lett. **348**, 89 (2001).
- [18] M. Pope and C. E. Swenberg, *Electronic Processes in Organic Crystals and Polymers* (Oxford University, New York, 1999), 2nd ed.
- [19]  $f_{\epsilon}(r_{\text{gp}}, T, F) = \frac{1}{2} \int_0^{\pi} d\theta \sin\theta e^{-(A+B)} \sum_{m,n=0}^{\infty} \frac{A^m B^{m+n}}{m!(m+n)!}$ ;  $A = 2q/r_{\text{gp}}$ ,  $B = \beta r_{\text{gp}}(1 + \cos\theta)$ ,  $q = e^2/8\pi\epsilon\epsilon_0 kT$ ,  $\beta = eF/2kT$  (see Ref. [18], p. 484). Averaging over  $\theta$  represents an isotropic blend morphology.
- [20] Internal field calculated as  $F = (\text{applied voltage} + x)/170 \text{ nm}$ ;  $x$  is the voltage corresponding to minimum  $-\Delta\text{PL}/\text{PL}$ , found to be 0.7 V (PFB:F8BT) and 0.3 V (TFB:F8BT) forward bias.
- [21] At temperatures below 230 K, the  $\Delta\text{PL}$  arising from the excitons’ Stark shift obscures the weak quenching signal.
- [22] B. J. Schwartz, Annu. Rev. Phys. Chem. **54**, 141 (2003), and references therein.